Sensitivity of atmospheric correction to loading and model of the aerosol

Cristiana Bassani[1], Federica Braga[2], Mariano Bresciani[3], Claudia Giardino[3], Maria Adamo[4], Cristina Ananasso[5], Luigi Alberotanza[2]

[1] Institute for Atmospheric Pollution Research (IIA), Italian National Research Council (CNR), Research Area of Rome 1, Via Salaria Km 29,300, 00016 Monterotondo Scalo, Rome, Italy
[2] Institute of Marine Sciences (ISMAR), Italian National Research Council (CNR), Arsenale Tesa 104, Castello 2737/F, 30123 Venice, Italy
[3] Institute for Electromagnetic Sensing of the Environment (IREA), Italian National Research Council (CNR), Via Bassini 13, 20133 Milan, Italy
[4] Institute of Intelligent Systems for Automation (ISSIA), Italian National Research Council (CNR), Via G. Amendola 122/D-O, 70126 Bari, Italy
[5] Earth Observation Unit (EO), Italian Space Agency (ASI), Via del Politecnico, 00133, Rome, Italy

cristiana.bassani@iia.cnr.it

Abstract

The physically-based atmospheric correction requires knowledge of the atmospheric conditions during the remotely data acquisitions [4, 8, 3, 2]. The effects of solar beam extinction in the atmospheric window of visible spectral domain are related to the aerosol loading, by the aerosol optical thickness at $\lambda = 550nm$ (τ_{550}) [5, 14, 8, 7], and also to the aerosol optical and micro-physical properties. Recently, the atmospheric correction of hyperspectral data is considered sensitive to the aerosol type, as reported in [1].Within the framework of CLAM-PHYM (Coasts and Lake Assessment and Monitoring by PRISMA HYperspectral Mission) project, funded by Italian Space Agency (ASI), the role of the aerosol on the accuracy of the atmospheric correction of hyperspectral image acquired over water target is investigated. In this work, the results of the atmospheric correction of HICO (Hyperspectral Imager for the Coastal Ocean) images acquired on Northern Adriatic Sea in the Mediterranean are presented. The atmospheric correction has been performed by an algorithm specifically developed for HICO sensor, HICO@cri (HICO atmospherically corrected reflectance image). The water reflectance, obtained from HICO@cri with variable optical properties and fixed loading of the aerosol, has been compared. The results highlight the requirements to define the aerosol characteristics, loading and type, to simulate the radiative field in the atmosphere system for an accurate atmospheric correction of hyperspectral data, improving the accuracy of the results for surface reflectance process over water, a dark-target.

1. Study area & Data

STUDY AREA

The Venice Lagoon ($45.4°N$, $12.508°$, in the Northern Adriatic Sea, Mediterranean basin) is a test site of the CLAM-PHYM project.

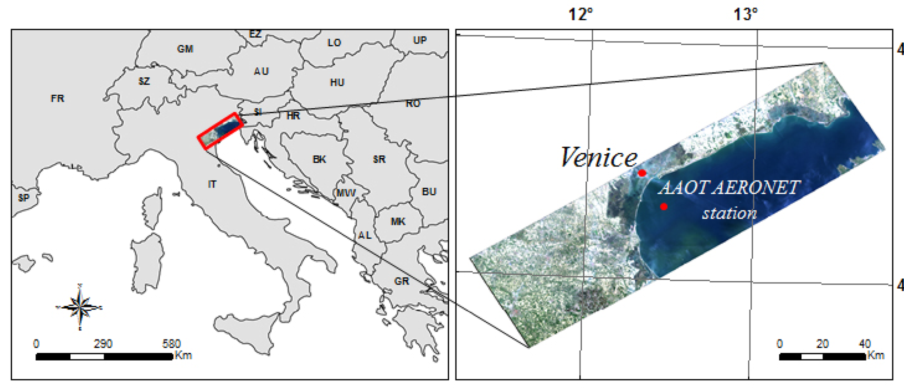

AEROSOL

The aerosol characterization has been performed by using CIMEL data available from AAOT AERONET site [11] and continental and maritime types [13, 6].

SATELLITE RADIANCE

The remotely sensed data have been acquired by the HICO sensor operating on the visible spectral domain [10]. HICO is now provided by NASA's International Space Station (ISS) Program.

2. Methods

2.1 Aerosol characterization

The aerosol loading can be measured by the τ_{550} available from AAOT AERONET site. The extinction and the absorption coefficients of the aerosol are defined by the single scattering albedo (ω_λ) and the angular distribution of scattered radiation is described by the asymmetry parameter (g_λ). These optical properties are available from the AAOT AERONET site and simulated for maritime and continental types by the 6SV radiative transfer code [13, 8, 14].

2.2 HICO@cri: HICO atmospherically corrected reflectance image

The HICO@cri algorithm dedicated to the atmospheric correction of HICO image, has been developed. The procedure takes into account the aerosol loading by the τ_{550} and the aerosol type by ω_λ and g_λ. The parameters of the data acquisition geometry are provided with the HICO image and considered in the algorithm. The HICO@cri agorithm retrieves the pixel reflectance, ρ_λ^{gnd}, by using the equation [12, 2]:

$$\rho_\lambda^{gnd} = \frac{t_\lambda^{gas}(\mu_s,\mu_v)\rho_\lambda^{atm} - \rho^{TOA}}{S_\lambda[t_\lambda^{gas}(\mu_s,\mu_v)\rho_\lambda^{atm} - \rho^{TOA}] - T_\lambda^{\downarrow}(\mu_s)T_\lambda^{\uparrow}(\mu_v)t^{gas}} \quad (1)$$

$\rho^{TOA} = \pi L_\lambda/\mu_s E_\lambda$ is the at-sensor reflectance; the L_λ is the at-sensor radiance; the $\mu_{s,v} = cos(\theta_{s,v})$ where $\theta_{s,v}$ are the solar (s) and viewing (v) zenith angles; E_λ is the solar irradiance at the Top Of Atmosphere (TOA); t_λ^g is the transmittance due to the gas absorption; ρ_λ^{atm} is the intrinsic atmospheric reflectance; $T_\lambda^{\uparrow}$ and $T_\lambda^{\downarrow}$ are the total upwelling and downwelling transmittance, both with direct and diffuse components; S_λ is the atmospheric spherical albedo.

The HICO@cri removes the adjacency effect by the empirical formula [12, 2]:

$$\rho_\lambda = \rho_\lambda^{gnd} + \frac{t_\lambda^{dif}(\mu_v)}{t_\lambda^{dir}(\mu_v)}\left[\rho_\lambda^{gnd} - <\rho_\lambda^{gnd}>\right] \quad (2)$$

Where $T_\lambda^{\uparrow} = t_\lambda{}^{dir}(\mu_v) + t_\lambda^{dif}(\mu_v)$, direct and diffuse component of upwelling trasmittance. All the radiative quantities are simulated by using 6SV code.

3. Results

The simultaneous HICO and AERONET data have been taken into account to analyze the influence of the aerosol type on the results of the atmospheric correction of HICO image. The Table shows the available data satisfying the previous requirement.

YYYY/MM/DD	HICO	CIMEL	Aerosol Optical Thickness, τ_{550}
2012/01/11	13:21	13:22	0.100 (Lev 2.0)
2012/03/09	13:42	13:22	0.049 (Lev 2.0)
2012/05/12	7:18	7:20	0.248 (Lev 2.0)

During the three HICO acquisitions, ω_λ and g_λ attest that the aerosol optical properties are similar to the maritime type, like shown in the figure. Thus, the aerosol can be considered nonabsorbing ($\omega_\lambda \sim 1$, [9]) and characterized by a g_λ less than the value of the continental type, usually implemented in the atmospheric correction algorithms.

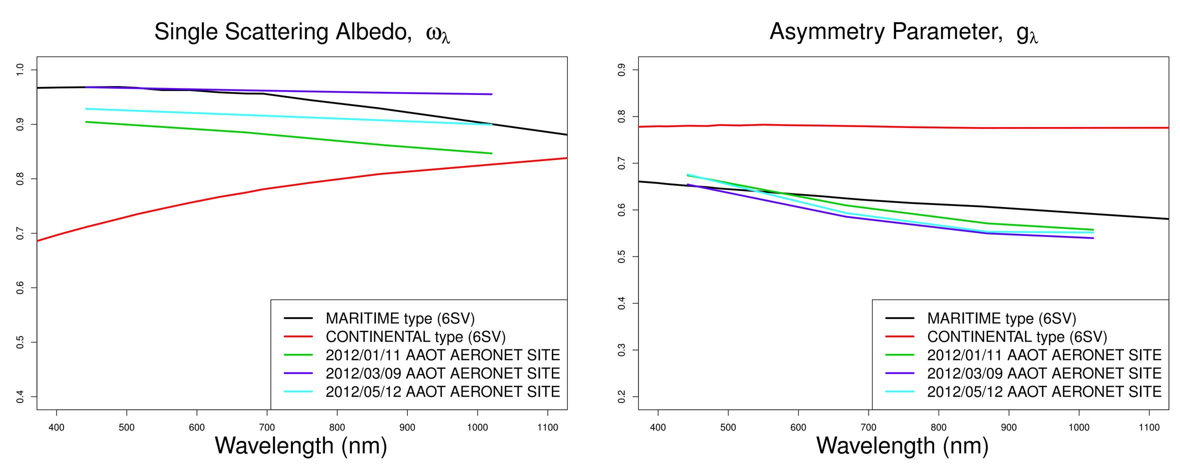

The HICO@cri algorithm has been applied to the above mentioned HICO images. The τ_{550} has been fixed to the AERONET value to avoid influence of the aerosol loading on the final reflectance, ρ_λ. The ω_λ and g_λ of AERONET site, and continental and maritime types have been considered. Thus, the surface reflectance of water pixel has been retrieved for fixed τ_λ and different optical properties. Examples are shown in the figure:

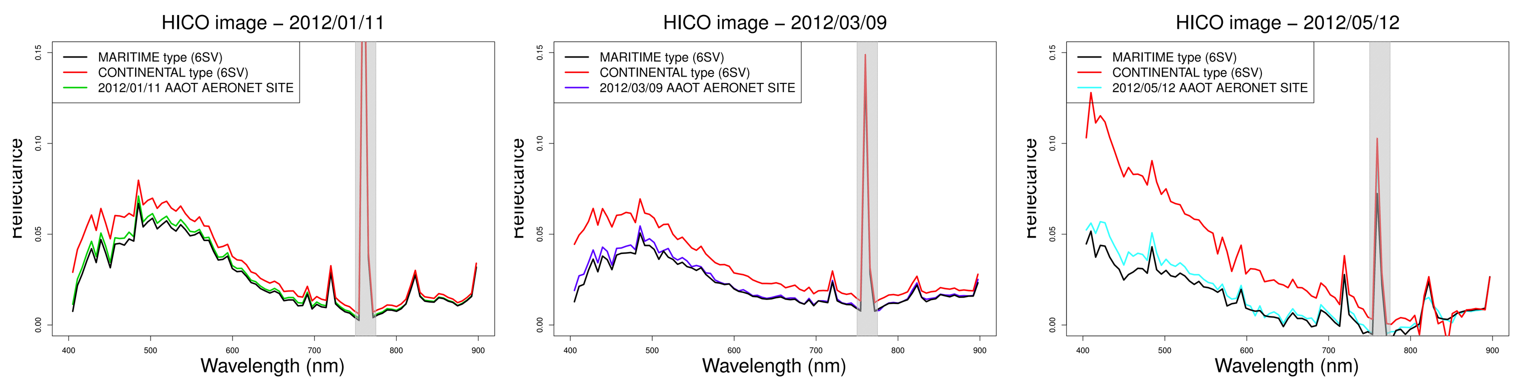

4. Conclusion

The study highlights the radiative effects of the aerosol types on the atmospheric correction of HICO image if a dark target is studied. As conclusion, the aerosol model plays a crucial role for an accurate physically-based atmospheric correction of hyperspectral data over water. Currently, the PRISMA mission provides valuable opportunities to study aerosol and their radiative effects on the hyperspectral data.

5. Acknowledgements

We thank the Dr. Zibordi, the principal investigator of AAOT AERONET station. This work is part of the CLAM-PHYM project, funded by ASI (Italian Space Agency).

References

[1] C. Bassani, R. Cavalli, and P. Antonelli, *Influence of aerosol and surface reflectance variability on hyperspectral observed radiance*, Atmospheric Measurement Techniques, 5 (2012), pp. 1139–1203.

[2] C. Bassani, R. M. Cavalli, and S. Pignatti, *Aerosol optical retrieval and surface reflectance from airborne remote sensing data over land*, Sensors, 10 (2010), pp. 6421–6438.

[3] B.-C. Gao, M. J. Montes, C. O. Davis, and A. F. H. Goetz, *Atmospheric correction algorithms for hyperspectral remote sensing data of land and ocean*, Remote Sensing of Environment, 113 (2009), pp. S17–S24.

[4] L. Guanter, V. Estellés, and J. Moreno, *Spectral calibration and atmospheric correction of ultra-fine spectral and spatial resolution remote sensing data. application to casi-1500 data*, Remote Sensing of Environment, 109 (2007), pp. 54–65.

[5] Y. J. Kaufman, D. Tanré, H. R. Gordon, T. Nakajima, J. Lenoble, R. Frouin, H. Grassl, B. M. Herman, M. King, and P. M. T. P.M., *Operational remote sensing of tropospheric aerosol over land from eos moderate resolution imaging spectroradiometer*, Journal of Geophysical Research, 102 (1997), pp. 17051–17067.

[6] A. A. Kokhanovsky, *Aerosol optics: light absorption and scattering by particles in the atmosphere*, Praxis Publishing Ltd, Chichester, UK, 2008.

[7] A. A. Kokhanovsky, J. L. Deuz, D. J. Diner, O. Dubovik, F. Ducos, C. Emde, M. J. Garay, R. G. Grainger, A. Heckel, M. Herman, I. L. Katsev, J. Keller, R. Levy, P. R. J. North, A. S. Prikhach, V. V. Rozanov, A. M. Sayer, Y. Ota, D. Tanr, G. E. Thomas, and E. P. Zege, *The inter-comparison of major satellite aerosol retrieval algorithms using simulated intensity and polarization characteristics of reflected light*, Atmospheric Measurement Techniques, 3 (2010), p. 909932.

[8] S. Y. Kotchenova, E. F. Vermote, R. Levy, and A. Lyapustin, *Radiative transfer codes for atmospheric correction and aerosol retrieval: Intercomparison study*, Applied Optics, 47 (2008), pp. 2215–2226.

[9] R. C. Levy, L. A. Remer, and O. Dubovik, *Global aerosol optical properties and application to moderate resolution imaging spectroradiometer aerosol retrieval over land*, Journal of Geophysical Research, 112 (2007), p. D13210.

[10] R. L. Lucke, M. Corson, N. R. McGlothlin, S. D. Butcher, D. L. Wood, D. R. Korwan, R. R. Li, W. A. Snyder, C. O. Davis, and D. T. Chen, *Hyperspectral imager for the coastal ocean: instrument description and first images*, Applied Optics, 50 (2011), pp. 1501–1516.

[11] F. Mélin, M. Clerici, G. Zibordi, and B. Bulgarelli, *Aerosol variaility in the adriatic sea from automated optical field measurements and sea-viewing wide fiel-of-view sensor (seawifs)*, Journal of Geophysical Research, 111 (2006), p. D22201.

[12] E. F. Vermote, N. E. Saleous, C. Justice, Y. Kaufman, J. Privette, L. Remer, J. Roger, and D. Tanré, *Atmospheric correction of visible to middle-infrared eos-modis data over land surfaces: Background, operational algorithm and validation*, Journal of Geophysical Research, 102 (1997), pp. 675–686.

[13] E. F. Vermote, D. Tanré, Deuzé, M. Herman, J. J. Morcrette, and S. Y. Kotchenova, *Second Simulation of a Satellite Signal in the Solar Spectrum - Vector (6SV)*, http://6s.ltdri.org, November 2006. 6S User Guide Version 3.

[14] E. F. Vermote, D. Tanré, J. L. Deuzé, M. Herman, and J. J. Morcrette, *Second simulation of the satellite signal in the solar spectrum, 6s: An overview*, IEEE Transactions on Geoscience and Remote Sensing, 35 (1997), pp. 675–686.